

## Shock Tube Rotational Relaxation Measurements in Low-Temperature Hydrogen

M. JOHN YODER

*Department of Physics, University of Michigan, Ann Arbor, Michigan 48104*

(Received 1 November 1971)

Rotational relaxation times are measured for normal hydrogen and parahydrogen in a cryogenic shock tube with initial temperatures of 80–100°K. A sensitive schlieren optical system, employing a laser light source and a photomultiplier, is used to measure laboratory relaxation times of the order of 0.1  $\mu$ sec, with a spatial resolution of 0.1 mm. Measurements are made over a temperature range of 140–450°K. Relaxation times are in general agreement with results obtained by other methods.

## INTRODUCTION

Although relaxation times have been extensively measured for shocks with dissociational, ionizational, and vibrational excitation modes, very little information is available concerning rotational relaxation times. Usually these times are so short that they are indistinguishable from the time necessary to achieve a Maxwellian distribution of particle velocities. This is due to the fact that the separation between adjacent energy levels is usually much less than  $\frac{3}{2}kT$ , the average energy of translation. Only in molecules with very small moments of inertia are the rotational energies sufficiently separated that their spacing is comparable to  $kT$ , thus leading to longer relaxation times. Even for the most favorable molecule, hydrogen, these times are still very short and difficult to measure. In the experiment reported a 1.17-m focal length schlieren optical system using a laser light source is used to detect very small density gradients. This system permits the use of low density test gas, leading to laboratory relaxation times sufficiently long to be measurable. Initial test-gas temperatures of 80–100°K are attained using a cryogenic shock tube which has been described elsewhere.<sup>1–3</sup>

## INTERNAL ENERGY SPECTRUM FOR MOLECULAR HYDROGEN

At temperatures less than 1000°K the hydrogen molecule behaves like a quantum mechanical rigid rotator. Only the ground vibrational state is populated. Thus the molecular energy levels,  $\epsilon_j$ , and degeneracies,  $g_j$ , can be written as

$$\epsilon_j = j(j+1)\hbar^2/2I, \quad (1)$$

$$g_j = 2j+1, \quad (2)$$

where  $I$  is the moment of inertia of the molecule and  $j$  is zero or any positive integer.

One must also consider the fact that hydrogen behaves as a mixture of two stable distinguishable components, orthohydrogen (nuclear spins parallel) and parahydrogen (nuclear spins opposed). Due to the Pauli exclusion principle, orthohydrogen may occupy only rotational states having odd  $j$  values, whereas parahydrogen may occupy only states having even  $j$  values. Normal hydrogen is a mixture of 25%

parahydrogen and 75% orthohydrogen. The percentage of parahydrogen can be increased to 100% by use of suitable techniques.<sup>1,4</sup>

The equilibrium populations of the rotational energy states are shown in Fig. 1 as a function of temperature. For initial shock tube temperatures below 80°K, only the ground state of each component is appreciably populated. In the high temperature gas behind the shock, the upper states become populated. At the temperatures of interest in this experiment, only a few rotational states are occupied. This experiment seeks to measure the time necessary for the change in excited-state populations behind the shock to approach to within  $1/e$  of that necessary for equilibrium.

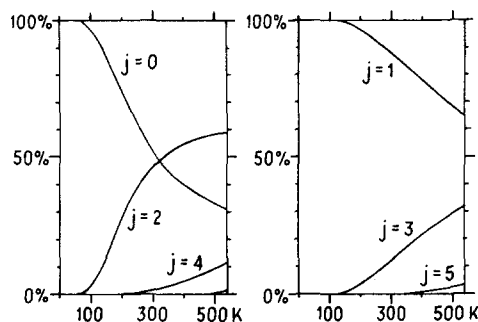


FIG. 1. Percentage population of rotational energy states for parahydrogen (left) and orthohydrogen (right).

## EXPERIMENTAL TECHNIQUE

A sensitive schlieren optical system is used to measure the density gradients near the shock. These measurements are made to look for a delay in the population of the excited rotational eigenstates. The population of these levels takes up translational energy from the gas, causing the temperature to decrease and the density to increase. A narrow source slit and 1.17-m focal length parabolic mirrors make it possible to detect very small density gradients. A spatial resolution of less than 0.1 mm is attained by use of a narrow vertical slit placed at the image of the test section. Behind the slit is an RCA 7265 photomultiplier, which is connected to an oscilloscope. The light beam is carefully oriented perpendicular to the

shock tube axis. These two narrow slits cause a very great decrease in the light reaching the photomultiplier, so a very bright light source is necessary if an adequate signal-to-noise ratio is to be obtained. The laser is an obvious choice. It is also useful for aligning the system, since the beam can be adjusted until the reflection from the windows coincides with the incident beam. A heavy interferometer housing is used as an optical bench for this arrangement to isolate the system from building vibrations.

### EXPERIMENTAL RESULTS AND INTERPRETATION

Schlieren density gradient profiles were obtained for parahydrogen, normal hydrogen, deuterium, and neon. Several shock profiles for normal hydrogen are shown in Fig. 2. The oscilloscope is triggered just before the image of the shock arrives at the photomultiplier slit. There is a sharp rise in the signal, followed by a somewhat slower decay. This slow decay is assumed to be caused by the finite time necessary to achieve equilibrium between the rotational and translational modes. In order to interpret these photomultiplier signals and infer a relaxation time from them, the relaxation processes and measurements must be examined in detail.

For a simple two-level gas of  $n$  particles the popula-

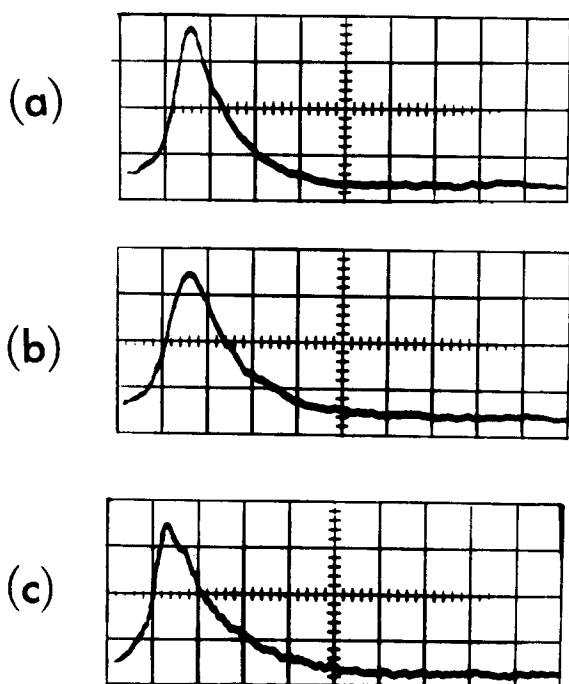


FIG. 2. Schlieren shock profiles in hydrogen. (a)  $P_0=1.55$  torr,  $T_0=98^\circ\text{K}$ ,  $T_1=410^\circ\text{K}$ , shock speed is 3.0 km/sec, oscilloscope sweep speed is 0.2  $\mu\text{sec}/\text{div}$ . (b)  $P_0=2.0$  torr,  $T_0=100^\circ\text{K}$ ,  $T_1=350^\circ\text{K}$ , shock speed is 2.4 km/sec, oscilloscope sweep speed is 0.2  $\mu\text{sec}/\text{div}$ . (c)  $P_0=4.0$  torr,  $T_0=83^\circ\text{K}$ ,  $T_1=130^\circ\text{K}$ , shock speed is 1.26 km/sec, oscilloscope sweep speed is 0.5  $\mu\text{sec}/\text{div}$ .

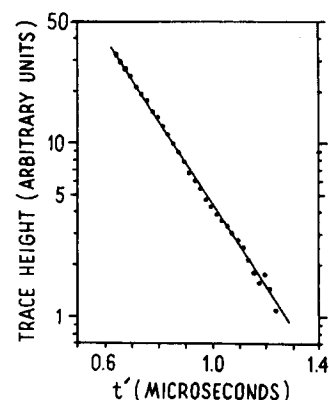


FIG. 3. Semilog plot of schlieren density gradient trace.

tions must obey the reaction equation,

$$dn_b/dt = k_{ab}n_a - k_{ba}n_b, \quad (3)$$

where  $n_a$  and  $n_b$  are the particle numbers in states  $a$  and  $b$ , respectively, and  $k_{ab}$  and  $k_{ba}$  are the probabilities per second of a transition  $a \rightarrow b$  and  $b \rightarrow a$ , respectively. The constraint  $n_a + n_b = n$  must be observed. So one obtains

$$(dn_b/dt) + (k_{ab} + k_{ba})n_b = k_{ab}n. \quad (4)$$

Assuming that  $k_{ab}$  and  $k_{ba}$  are constants independent of  $n_a$  and  $n_b$ , this differential equation has the solution

$$n_b = [k_{ab}n / (k_{ab} + k_{ba})] [1 - \exp(-t/\tau)], \quad (5)$$

where the relaxation time has the value

$$\tau = (k_{ab} + k_{ba})^{-1}. \quad (6)$$

The initial condition  $n_b = 0$  at  $t = 0$  has been assumed, but the same exponential would appear for any initial population of state  $b$ .

The constants  $k_{ab}$  and  $k_{ba}$  are related since the stationary equilibrium populations are given by the Boltzmann distribution law. Thus

$$dn_b^{eq}/dt = 0 = k_{ab}n_a^{eq} - k_{ba}n_b^{eq}, \quad (7)$$

with

$$n_a^{eq}/n_b^{eq} = (g_a/g_b) \exp[(\epsilon_b - \epsilon_a)/kT].$$

The relaxation time can thus be written

$$\tau = \{1 + (g_a/g_b) \exp[(\epsilon_b - \epsilon_a)/kT]\}^{-1} (k_{ab})^{-1}. \quad (8)$$

Since rotational transitions are caused primarily by binary molecular collisions,  $k_{ab}$  should be proportional to the collision frequency  $\nu_C$ , and

$$k_{ab} = \nu_C F(T). \quad (9)$$

At a fixed temperature,  $\nu_C$  is proportional to the pressure  $P$ . Thus the relaxation time may be written

$$\tau = G(T)/P. \quad (10)$$

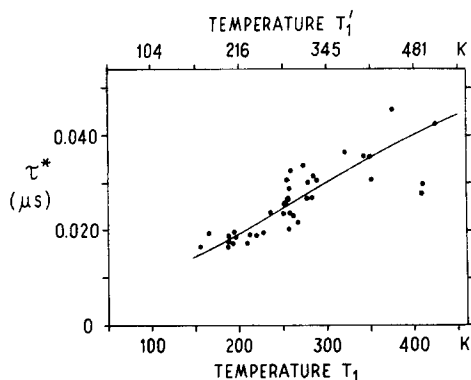


FIG. 4. Relaxation times for normal hydrogen as a function of temperature.

The form of  $G(T)$  is not obvious and must be determined experimentally or by a complex calculation.<sup>5</sup> The purpose of this experiment is to measure  $G(T)$  for normal hydrogen and parahydrogen. These are both, to a very good approximation, two-level gases for temperatures less than about 400°K.

In order to extract the relaxation time,  $\tau$ , from the data, the "relaxation tail" is plotted on a semilog plot as shown in Fig. 3. The plot is begun at the point at which the image of the shock leaves the slit of the photomultiplier. The slope of such a graph determines a laboratory relaxation time,  $\tau'$ , which is, however, not  $\tau$  as defined in Eq. (5). The laboratory relaxation time must be multiplied by the value of the density ratio across the shock to obtain  $\tau$ . This corrects for the fact that the gas seen at time  $t'$  after the passage of the shock was actually shock heated a longer time,  $t$ , where

$$t = (\rho_1/\rho_0)t'. \quad (11)$$

The measured relaxation times are converted to the

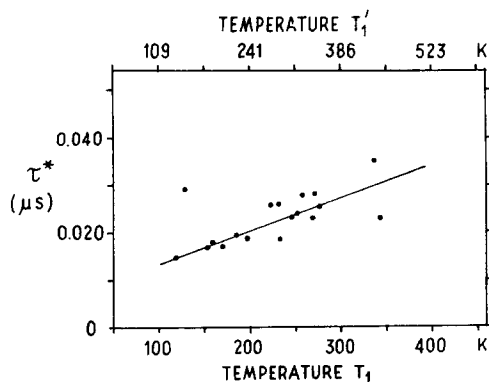


FIG. 5. Relaxation times for parahydrogen as a function of temperature.

standard form of those expected for one atmosphere pressure,  $\tau^*$ , using Eq. (10).

The results of the rotational relaxation measurements are shown in Fig. 4 for normal hydrogen and Fig. 5 for parahydrogen. Relaxation times,  $\tau^*$ , are determined for the temperature range 140–450°K. Initial pressures vary from 1.5 to 5.0 torr and are distributed over the entire temperature range. The relaxation times,  $\tau^*$ , for each temperature are inversely proportional to the pressure. This can be seen in Fig. 6 where the deviation of the relaxation times,  $\tau^*$ , from the mean values is plotted as a function of the pressure.

No measurable difference between rotational relaxation times in parahydrogen and normal hydrogen has been observed. This is consistent with previous experimental results and theoretical predictions. There is, however, a difference of as much as 20% in laboratory relaxation times for these two gases, due to the differences in their density ratios.

These results can also be written in terms of  $Z$ , the number of collisions necessary for the gas to relax to

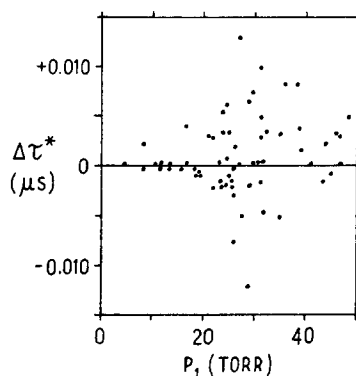


FIG. 6. Deviation of relaxation times from mean values as a function of the pressure behind the shock.

within  $1/e$  of its equilibrium value. Using collision frequency data given by Herzfeld and Litovitz,<sup>6</sup>  $Z$  varies from 370 collisions at 200°K to 440 collisions at 350°K.

Several shots were made in monatomic gases. No asymmetry is observed, as can be seen in the shock profiles shown in Fig. 7. This is expected, since no relaxation processes of any kind occur at these temperatures. The shock profiles are broader in time than those in hydrogen, due to the difference in shock speeds. In terms of the spatial thickness, these neon shocks are comparable to hydrogen shocks. The finite width of these profiles is caused primarily by shock curvatures, instrumental slitwidths, beam misalignment, and diffraction effects.

Shock profiles in deuterium show a tail similar to that of hydrogen. This is also expected, since ultrasonic experiments indicate that rotational relaxation times for deuterium are comparable to those for hydrogen.

## ERRORS

The error due to pressure measurement uncertainty is insignificant. Also negligible are the effects of the  $\pm 1^\circ\text{K}$  initial-temperature measurement errors and nonuniformities. Research-grade hydrogen is used, and leak rates into the vacuum system are less than  $2 \mu/\text{min}$ . It is believed that impurities do not contribute significantly to the scatter of the experimental points. The rise and fall times of the electronic circuits were calculated and measured to be less than  $0.02 \mu\text{sec}$ ; errors from this source are also small.

The largest uncertainties are probably introduced through the diffraction of the monochromatic laser light from the shock and the necessity of making measurements very close to the shock. It is not always possible to determine accurately the point at which the shock image leaves the photomultiplier slit and the relaxation tail begins. Additionally, some shots show evidence of shock curvature and boundary layer effects. It is noteworthy that the scatter of the experimental points is not very large for shocks with low final temperatures. For these lower strength shocks, laboratory relaxation times are longer due to the smaller value of the density ratio, and the shock curvature is less pronounced due to the higher initial pressures used.

The actual temperature of the gas during the relaxation process is always higher than the final equilibrium temperature,  $T_1$ . The temperature of the shock heated gas, before any rotational relaxation has taken place, is called  $T_1'$ . Values of  $T_1'$  compared to  $T_1$  are shown in Figs. 4 and 5. Errors introduced by ignoring this temperature nonuniformity are small compared to other errors in the experiment.

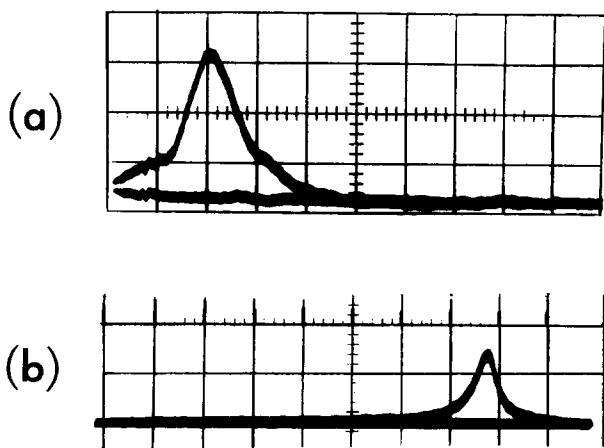


FIG. 7. Schlieren shock profiles in neon. (a)  $P_0=3.0$  torr,  $T_0=86^\circ\text{K}$ ,  $T_1=564^\circ\text{K}$ , mach No. is 4.3, oscilloscope sweep speed is  $0.5 \mu\text{sec}/\text{div}$ . (b)  $P_0=3.0$  torr,  $T_0=97^\circ\text{K}$ ,  $T_1=1139^\circ\text{K}$ , mach No. is 5.8, oscilloscope sweep speed is  $1.0 \mu\text{sec}/\text{div}$ .

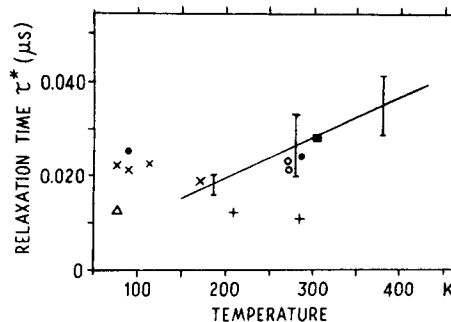


FIG. 8. Comparison of mean values of this experiment with other experimental results. —, this experiment; ■, Huber and Kantrowitz<sup>8</sup>; ○, Stewart and Stewart; ●, Van Itterbeek; +, Huber and Kantrowitz<sup>8</sup>; △, ×, Jonkman *et al.*<sup>10</sup>

## COMPARISON WITH OTHER EXPERIMENTS

A lower limit for relaxation times of about  $1.1 \times 10^{-8}$  sec was obtained by Hornig and Green<sup>7</sup> by measuring the reflectivity of a light beam obliquely incident on a shock. Huber and Kantrowitz<sup>8</sup> measured relaxation times using an impact tube. Rotational relaxation times have also been inferred from numerous measurements of ultrasonic absorption and dispersion in hydrogen by Van Itterbeek, Stewart, Rhodes, Jonkman, and others.<sup>5,9,10</sup> The comparison of these results<sup>6</sup> with the mean values of relaxation times obtained in this experiment are shown in Fig. 8. There is general agreement with ultrasonic measurements and the value from the impact tube measurement of Huber and Kantrowitz as given in Ref. 6. There is, however, an unexplained disagreement with the relaxation times as given in the original impact tube reference.<sup>8</sup>

## CONCLUSIONS

The asymmetry shown in the shock profiles is due to rotational relaxation phenomena. This is confirmed by the following observations:

- (1) The decay of the photomultiplier signal is exponential.
- (2) The expected inverse proportionality of relaxation times to pressure is observed.
- (3) There is no asymmetry of the shock profiles for neon or argon.
- (4) The measured relaxation times are consistent with those obtained by other methods.

Although the scatter of experimental points is too large to constitute an accurate measurement of relaxation times for high temperatures, it is believed that the results for temperatures less than  $250^\circ\text{K}$  are relatively precise. The measurements for high temperatures are valuable in spite of the scatter of points, since they provide a simple and direct confirmation of previous results.

## ACKNOWLEDGMENTS

This research formed part of a Ph.D. dissertation performed in the laboratory of Professor Otto Laporte. I would like to express my appreciation for his advice and encouragement. This work was supported by the United States Air Force Office of Scientific Research.

<sup>1</sup> M. J. Yoder, Ph.D. thesis, University of Michigan and University of Michigan Tech. Rept. 032150-1-T, 1971.

<sup>2</sup> M. J. Yoder, "Shock Waves in Low Temperature Parahydrogen and Normal Hydrogen," Phys. Fluids (to be published).

<sup>3</sup> O. Laporte and M. J. Yoder, Proc. Intern. Symp. Shock Tube 8th, London, 1971.

<sup>4</sup> A. Farkas, *Orthohydrogen, Parahydrogen, and Heavy Hydrogen* (Cambridge U. P., Cambridge, England, 1935).

<sup>5</sup> K. Takayanagi, Progr. Theoret. Phys. (Kyoto) Suppl. 25, 1 (1963).

<sup>6</sup> K. F. Herzfeld and T. A. Litovitz, *Absorption and Dispersion of Ultrasonic Waves* (Academic, New York, 1959).

<sup>7</sup> E. F. Greene and D. F. Hornig, J. Chem. Phys. 21, 617 (1953).

<sup>8</sup> P. W. Huber and A. Kantrowitz, J. Chem. Phys. 15, 275 (1947).

<sup>9</sup> A. B. Bhatia, *Ultrasonic Absorption* (Oxford U. P., London, 1967).

<sup>10</sup> R. M. Jonkman, G. J. Prengsma, and J. J. M. Beenakker, Proc. Intern. Symp. Rarefied Gas Dyn., 5th, Cambridge, Mass., 1968 (1969).

Shock Tube Vibrational Relaxation Measurements: N<sub>2</sub> Relaxation by H<sub>2</sub>O and the CO-N<sub>2</sub> V-V Rate

C. W. VON ROSENBERG, JR.,\* K. N. C. BRAY, AND N. H. PRATT

*Department of Aeronautics and Astronautics, The University of Southampton, Southampton, England*

(Received 8 March 1971)

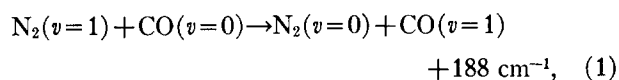
Shock tube measurements of the rates of vibrational relaxation of N<sub>2</sub> by H<sub>2</sub>O and the vibrational exchange between N<sub>2</sub> and CO are described. Simultaneous measurements of H<sub>2</sub>O  $\nu_2$  band and CO fundamental band ir emission were performed in mixtures of 1%-10% CO+~1% H<sub>2</sub>O+N<sub>2</sub>. Measurement of H<sub>2</sub>O emission by a calibrated optical system allowed an accurate determination of the concentration of H<sub>2</sub>O for each run. The CO emission had two, almost decoupled, regions of behavior which allowed determination of two relaxation times:  $P\tau_{NC} \approx 1.6 \text{ atm} \cdot \mu\text{sec}$  ( $V-V$  exchange relaxation time between N<sub>2</sub> and CO) and  $P\tau_{NH} \approx 1.5 \text{ atm} \cdot \mu\text{sec}$  ( $T-V$  relaxation of N<sub>2</sub> by H<sub>2</sub>O), both for  $960 < T < 2200^\circ\text{K}$ .

## I. INTRODUCTION

Water vapor produces a large reduction in the observed vibrational relaxation time of nitrogen.<sup>1-3</sup> Quantitative measurement of this rate however has been difficult because adsorption of H<sub>2</sub>O onto solid surfaces can cause an uncertainty in knowing its gas phase concentration. In earlier papers,<sup>4,5</sup> we described a technique which resolved this problem for high temperature shock tube measurements, by quantitatively measuring [H<sub>2</sub>O] immediately following the vibrational relaxation. This technique was used in measurements<sup>5</sup> to determine the effect of water vapor on the vibrational relaxation of CO. Herein we report extensions of our earlier work by describing experiments on CO+N<sub>2</sub>+H<sub>2</sub>O mixtures from which we obtain the rate of vibrational deactivation of N<sub>2</sub> by H<sub>2</sub>O as well as the rate of vibration-vibration exchange between N<sub>2</sub> and CO.

Because of the moderately close CO-N<sub>2</sub> vibrational energy resonance and therefore rapid vibrational energy exchange, we planned to use CO as a tracer species to reflect the N<sub>2</sub> vibrational energy as it relaxed in the presence of water vapor. This approach has been successfully used previously<sup>6</sup> in mixtures of 1% CO+N<sub>2</sub> to measure the vibrational relaxation of N<sub>2</sub> by N<sub>2</sub>. Because of the physical similarity of CO and N<sub>2</sub>, one might expect the vibrational relaxation

time of N<sub>2</sub> by H<sub>2</sub>O ( $\tau_{NH}$ ) to be comparable to that for CO relaxation by H<sub>2</sub>O ( $\tau_{CH}$ ). We found however that  $\tau_{NH} \approx 10 \times \tau_{CH}$  and that the vibration-vibration ( $V-V$ ) relaxation time ( $\tau_{NC}^e$ ) for the single quantum exchange



is of the same order of magnitude as  $\tau_{NH}$ . As will be explained, this resulted in the CO signal having two, almost decoupled, regions of behavior as it approached equilibrium; analysis of the signals enabled us to deduce both  $\tau_{NH}$  and  $\tau_{NC}^e$ .

## II. EXPERIMENTAL

Complete details of the equipment and operating and calibration procedures may be found in Refs. 4 and 5; nothing has been changed following Ref. 5 so that only a brief description is given here.

Experiments were performed in a 5-in. i.d. stainless steel shock tube having a net leak plus outgassing rate of  $< 10^{-3}$  torr/min. Measurements were made behind incident shocks of CO fundamental band (4.0-4.9  $\mu$ ) and H<sub>2</sub>O  $\nu_2$ -band (6.3-11  $\mu$ ) emission by two optical systems employing simple reflective optics, interference filters, and fast response infrared detectors. The H<sub>2</sub>O system was calibrated, for the optically